

# A Stability Measure for Underconstrained Cable-Driven Robots

Paul Bosscher  
Woodruff School of Mech. Eng.  
Georgia Institute of Technology  
Atlanta, Georgia 30332-0405, USA  
Email: paulbosscher@hotmail.com

Imme Ebert-Uphoff  
Woodruff School of Mech. Eng.  
Georgia Institute of Technology  
Atlanta, Georgia 30332-0405, USA  
Email: ebert@me.gatech.edu

**Abstract**—This paper introduces a slope-based measure of the stability of a pose of an underconstrained cable robot. In order to define this measure, the set of twists that the end-effector can instantaneously undergo is found. The measure is then derived using an energy-based approach to generalize the definition of slope for mixed-dimensional twists. In order to more easily understand and calculate the measure an intermediate space is introduced. An example is worked out for a sample manipulator and the stability measure is used to define a measure of overall manipulator stability.

## I. INTRODUCTION

Cable-driven robots, referred to as cable robots in this paper, are a type of robotic manipulator that has recently attracted interest for large workspace manipulation tasks. Cable robots are relatively simple in form, with multiple cables attached to a mobile platform or end-effector as illustrated in Figure 1. The end-effector is manipulated by motors that can extend or retract the cables. These motors may be in fixed locations or mounted to mobile bases. The end-effector may be equipped with various attachments, including hooks, cameras, electromagnets and robotic grippers. Figure 1 illustrates a cable robot with four cables equipped with a robotic gripping tool grasping a barrel.

Cable robots possess a number of desirable attributes which make them well-suited for a variety of applications. Because the motors may reel out a large amount of cable they can have very large workspaces. Because the motors do not need to be mounted near the end-effector they are suitable for operating in hazardous environments. Their load capacity can be very high, in some cases comparable to construction cranes. Their high payload-to-weight ratio makes them attractive for high-speed manipulation tasks. Their simple design makes them inexpensive, modular, transportable and easily reconfigurable.

Despite these characteristics, there have been relatively few cable robots used in practical applications. Three examples of cable robots that are currently in use are the Skycam [1], Intelligent Spreader Bar [2] and the NIST RoboCrane [3]. The Skycam is a broadcast-quality robotic camera suspended from a cable-driven computerized transport system with joystick control and is used in stadiums and indoor arenas. The Intelligent Spreader Bar is a six-cable spatial cable robot designed for transferring cargo at sea from one ship to another. The NIST RoboCrane is a large-workspace robot for material handling in warehouses and storage facilities.

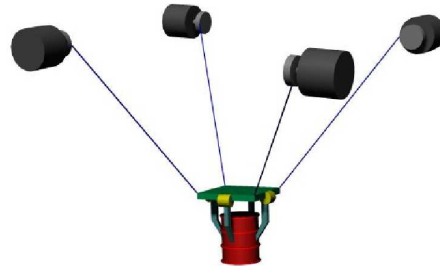


Fig. 1. Example Cable Robot.

Cable robots can be divided into two types: fully constrained and underconstrained. In the fully constrained case the pose (position and/or orientation) of the end-effector can be completely determined given the current lengths of the cables. In contrast, underconstrained manipulators use fewer cables than fully constrained manipulators and thus the pose of the end-effector is not completely determined by the lengths of the cables. Instead, these manipulators rely on the presence of gravity to determine the resulting pose of the end-effector. While this complicates the forward kinematics of underconstrained cable robots, it decreases problems with cable interference. For example, the manipulator in Figure 1 uses only four cables in order to decrease the likelihood of cable interference and as a result is underconstrained. In fact, the Skycam, Intelligent Spreader Bar and NIST RoboCrane are all underconstrained. This paper will deal specifically with underconstrained cable robots.

Because underconstrained cable robots are not fully constrained and must rely on gravity to determine the pose of the end-effector, it is possible for the pose of the end-effector to be changed by the presence of external disturbances. Due to the likelihood that these external disturbances cannot be completely predicted, the possibility arises that the resulting pose of the manipulator cannot be known. Such a situation will cause problems in many applications and thus should be avoided. It is therefore of interest to investigate the stability of underconstrained cable robots in order to avoid situations where disturbances change the pose of the end-effector. To this end, a stability measure has been developed for underconstrained cable robots and will be presented in this paper.

The organization of this paper is as follows: Section II

discusses some related work, Section III discusses stability and motivates the resulting stability measure, Section IV discusses stability in the context of the end-effector’s constraint surface, Section V presents the stability measure, Section VI discusses calculation of the stability measure, Section VII briefly presents some applications of the stability measure, Section VIII discusses the pros and cons of this approach and Section IX presents some conclusions and future work.

## II. RELATED WORK

While a number of researchers have developed analytical tools for cable robots, none have dealt specifically with the stability of underconstrained cable robots. Most have dealt with issues of workspaces ([4], [5], [6]), manipulability ([7], [8], [9]) and control ([10], [11]). The authors have investigated the set of external wrenches that can be opposed by a cable robot [12], but that study relies on a more explicit knowledge of the external disturbances.

There is a topological similarity between cable robots and problems in fixturing and robot grasping that has been pointed out by [13], [14] and [15]. This similarity arises because cables can pull but not push on the end-effector, while fixture contacts and robot finger contacts can push but not pull on an object. Grasp stability has been studied in great detail (for example [16], [17]). However, these studies have often included the effects of friction at the contact points, an effect that is not truly present in cable robots. The remaining studies typically focus on fixtures or grasps that fully constrain the object. Thus the majority of the research to date on fixture and grasp stability does not transfer easily to the stability of underconstrained cable robots.

## III. STABILITY

As was stated in Section I, it is of interest to investigate the stability of underconstrained cable robots. In the stability analysis presented here, it is assumed that all cables are ideal; that is, they have negligible mass, no upper tension limit and do not stretch or sag. The motor systems reeling the cables in and out are assumed to have no upper limit on the cable tension that can be provided and the locations of the attachments of the cables to the motors are known. The end-effector is assumed to be a single rigid body with known locations of cable attachment points and known inertial properties. Cable lengths are assumed to be known and the presence and direction of gravity are assumed to be known. External disturbances are assumed to be unknown wrenches (force/moment combinations) of unknown magnitudes that act only on the end-effector.

For now, stability will be defined in general terms as “the likelihood that an external disturbance will disturb the end-effector from a given equilibrium pose.” In other words, a manipulator with high stability has a relatively high ability to resist external disturbances. Note that here stability is associated with a particular pose of the manipulator. Determining the overall stability of a manipulator will be discussed in Section VIII. Note also that the analysis presented here is

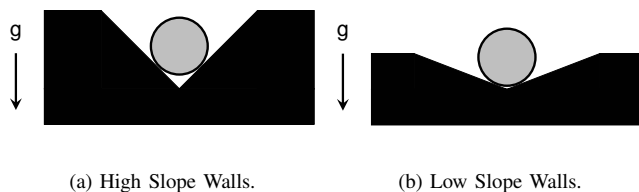


Fig. 2. Round Object Fixtured in a V-Block

based on *infinitesimal stability*, where the properties of the manipulator are only considered at the equilibrium pose and for infinitesimal motion of the end-effector. This is in contrast to *finite stability*, where the manipulator stability is examined through finite displacement of the end-effector.

While the majority of the research to date on fixture and grasp stability does not transfer easily to the stability of underconstrained cable robots, the topological similarity between these problems motivates looking at fixtures and grasps that rely on gravity in order to constrain an object. Consider the scenario shown in Figure 2. Here two identical round objects rest in two different V-blocks and each object is held in place by the frictionless contacts with the V-block walls and the influence of gravity. For the sake of this example let us neglect the rotation of the objects and consider only translation. The fixtures do not provide complete constraint, thus the objects cannot resist any arbitrary disturbances. However it is obvious that because the V-block in Figure 2(a) has steeper walls than the V-block in Figure 2(b), the object in Figure 2(a) is less likely to move given a random external disturbance, and thus is more stable. From this simple example it is clear that the stability of the object depends on the slope (with respect to gravity) of the constraint surfaces that restrict its motion. In addition, if a V-block had two walls with two different slopes the stability of the fixture is dominated by whichever wall has the lowest slope. Thus for this example the stability is a function of the lowest slope of the constraint surfaces that contact the object.

This concept can be extended to cable robots. The cables impose uni-directional constraints on the end-effector that locally are similar to V-block walls. A simple example is shown in Figure 3, where the end-effector is a point mass. The constraint surfaces are shown as the dashed arcs, where the end-effector must lie in the shaded region between the arcs. The vectors  $\vec{v}_1$  and  $\vec{v}_2$  are tangent to the constraint surfaces at their intersection (the location of the end-effector) and the slopes of the vectors are  $s_1$  and  $s_2$ , respectively. Note that all slopes will be considered in the positive sense (i.e.  $s_1 = \frac{|v_{1,y}|}{|v_{1,x}|}$ ). The stability of this pose of the robot is analogous to a point object fixtured in a block with walls shaped like the dashed arcs. The likelihood of the end-effector being disturbed from this pose will then be determined by the slope of the constraint surfaces with respect to gravity at the point where it is currently contacting the constraint surfaces. Thus for this manipulator the stability of the manipulator pose is determined

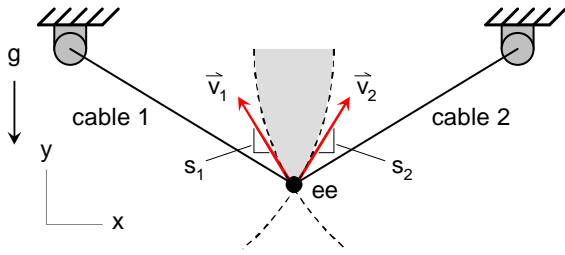


Fig. 3. Planar point-mass cable robot with constraint surfaces.

by the smaller of  $s_1$  and  $s_2$ .

Using slope as a stability measure has several advantages. In addition to being physically meaningful and easy to visualize, it is scale- and frame-invariant. However, attempting to extend this concept of slope-based stability to a general stability measure introduces two significant challenges. First, in order to evaluate the stability of a pose in this manner it is necessary to form the local constraint surface for a general underconstrained cable robot. This will be discussed in Section IV. Second, for the case where the end-effector is not a point mass it is necessary to define what is meant by the “slope” of a surface in mixed-dimensional space. This will be addressed in Section V, leading to the definition of a stability measure that is applicable in mixed-dimensional spaces.

#### IV. UNCONSTRAINED TWISTS

Forming the complete constraint surface for a particular pose of an underconstrained cable robot can be very difficult. However, for the purpose of this first-order analysis it is only necessary to form the constraint surface locally, that is, in an infinitesimal sense. Because the local constraint surface only limits the infinitesimal displacement of the end-effector, it is appropriate to think of the constraint surface as providing a constraint on the instantaneous twists (combinations of linear and angular velocity) that the end-effector could be given at this pose. Thus the effects of the local constraint surface can be examined by forming the set of all twists that the end-effector can undergo instantaneously without violating the constraints imposed by the cables. This set will be referred to as the set of *unconstrained twists*,  $U$ .

The set  $U$  can be formed by analysis of the Jacobian matrix of the robot. The Jacobian matrix  $\mathbf{J}$  defines the linear relationship between the velocities of the cables extending or retracting ( $\dot{q}_1 \dots \dot{q}_m$ ) and the resulting twist of the end-effector  $\mathcal{S}^t = (\vec{v}_{ee} \ \vec{\omega}_{ee})$ :

$$\begin{pmatrix} \dot{q}_1 \\ \vdots \\ \dot{q}_p \end{pmatrix} = \mathbf{J} \mathcal{S}^t \quad (1)$$

where the rows of  $\mathbf{J}$  are pure-force wrenches along the cables:

$$\mathbf{J} = [\mathcal{S}_1^w \ \dots \ \mathcal{S}_p^w]^T. \quad (2)$$

Here  $\mathcal{S}_i^w$  is the screw along the  $i^{\text{th}}$  cable:

$$\mathcal{S}_i^w = \begin{pmatrix} \vec{u}_i \\ \vec{c}_i \times \vec{u}_i \end{pmatrix} \quad (3)$$

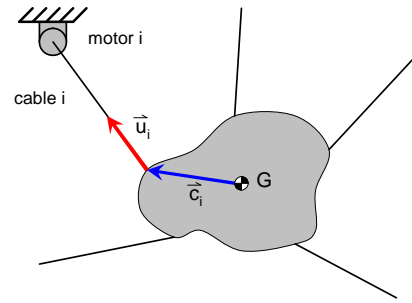


Fig. 4. Diagram of Kinematic Parameters.

where  $\vec{u}_i$  is the unit vector running along cable  $i$  directed away from the end-effector,  $\vec{c}_i$  is the vector from  $G$ , the center of gravity of the end-effector, to the point on the end-effector where cable  $i$  is connected as illustrated in Figure 4 and there are  $p$  cables attached to the end-effector. Note that  $\dot{q}_i > 0$  corresponds to the  $i^{\text{th}}$  cable being reeled in. For this Jacobian relationship to hold all cables must remain in tension.

Based on  $\mathbf{J}$ , the set of unconstrained twists  $U$  can be formed. A method will be presented first for determining  $U$  when the manipulator is not redundant. A cable robot is non-redundant when  $p \leq n$ , where  $n$  is the dimension of the task space, and thus  $\mathbf{J}^T$  has no nullspace (i.e. the wrenches  $\mathcal{S}_1^w, \dots, \mathcal{S}_p^w$  are linearly independent). After the method is presented, it will be discussed briefly how the method must be modified for redundant manipulators.

The set  $U$  consists of two subsets of twists, termed *Bi-Directional Unconstrained Twists* and *Uni-Directional Unconstrained Twists*. These subsets can be formed by examining the nullspace of  $\mathbf{J}$  and the nullspaces of modified  $\mathbf{J}$ 's, respectively.

##### A. Bi-Directional Unconstrained Twists

In order to find the bi-directional unconstrained twists, it is necessary to determine whether  $\mathbf{J}$  has a nontrivial nullspace. If it does, that means that there exists a twist that the end-effector can instantaneously undergo without violating any cable constraints or causing any of the cables to go slack. If  $p < n$ , this will always be the case regardless of the location of the end-effector within the workspace. If, however,  $p \geq n$ , a nontrivial nullspace of the Jacobian means that the manipulator is in a configuration where the constraints imposed by the cables have degenerated due to the geometry of the pose. Such a situation has been termed a “wrench deficiency” of a cable robot [12], and is very similar to a singularity of a parallel robot.

Regardless, if a nontrivial nullspace of  $\mathbf{J}$  exists of dimension  $r$ , then a set of  $r$  linearly independent twists that span the nullspace of  $\mathbf{J}$  can be formed and labelled  $\mathcal{S}_{bi,1}^t$  through  $\mathcal{S}_{bi,r}^t$ . These twists are bi-directional unconstrained twists, so named because the end-effector can move in either the positive or negative direction,  $\mathcal{S}_{bi,j}^t$  or  $-\mathcal{S}_{bi,j}^t$ , without violating a cable constraint. The span of these twists forms the complete set of all bi-directional unconstrained twists.

### B. Uni-Directional Unconstrained Twists

The remaining elements of  $U$  are uni-directional unconstrained twists, which cause one or more cables to go slack. In order to form the uni-directional twists, sub-matrices of the Jacobian must be formed. First we form the Jacobian matrix,  $\mathbf{J}_{mod,i}$ , that would result if the  $i^{th}$  cable were removed by removing the  $i^{th}$  row of  $\mathbf{J}$ :

$$\mathbf{J}_{mod,i} = [\$1^w \dots \$_{i-1}^w \ \$_{i+1}^w \dots \$p^w]^T, \quad i = 1, \dots, p \quad (4)$$

The nullspace of this modified matrix  $\mathbf{J}_{mod,i}$  is one dimension higher than the original nullspace of  $\mathbf{J}$ . A new twist, termed  $\$_{uni,i}^t$ , can be constructed such that the set of twists  $\{\$_{uni,i}^t \ \$_{bi,1}^t \dots \$_{bi,r}^t\}$  spans the nullspace of  $\mathbf{J}_{mod,i}$  and  $(\$i^w)^T \$_{uni,i}^t > 0$ .

If the end-effector undergoes any twist  $\alpha \$_{uni,i}^t$ , where  $\alpha$  is a scalar, then if  $\alpha > 0$  cable  $i$  will go slack, if  $\alpha < 0$  the constraint imposed by cable  $i$  is violated, and if  $\alpha = 0$  cable  $i$  remains taut. This is the source of the name ‘‘uni-directional unconstrained twist,’’ because  $\alpha \$_{uni,i}^t$  is an instantaneously permissible motion only if  $\alpha \geq 0$  (i.e. the motion along the twist is permitted in only one direction). This can be easily verified by noting that

$$\mathbf{J} \{ \alpha \$_{uni,i}^t \} = \alpha \begin{bmatrix} (\$1^w)^T \\ \vdots \\ (\$p^w)^T \end{bmatrix} \$_{uni,i}^t = \alpha \begin{bmatrix} 0 \\ \vdots \\ 0 \\ (\$i^w)^T \$_{uni,i}^t \\ 0 \\ \vdots \\ 0 \end{bmatrix} = \begin{bmatrix} 0 \\ \vdots \\ 0 \\ \dot{q}_i \\ 0 \\ \vdots \\ 0 \end{bmatrix} \quad (5)$$

where  $\dot{q}_i$  is the velocity at which cable  $i$  must be reeled in ( $\dot{q}_i > 0$ ) or out ( $\dot{q}_i < 0$ ) in order to keep the cable taut. Thus if all cable lengths are held fixed,  $\alpha < 0$  would result in the cable needing to be reeled out, thus the cable constraint is being violated and  $\alpha > 0$  would result in the cable needing to be reeled in, thus the cable will go slack.

This procedure can be repeated for each of the cables, where the nullspace of  $\mathbf{J}_{mod,i}$  is used to form the twist  $\$_{uni,i}^t$ , resulting in the set of twists  $\{\$_{uni,1}^t \dots \$_{uni,p}^t\}$ .

### C. Forming $U$

It can be shown that the set of all unconstrained twists  $U$  can then be described as:

$$U = \{ \$^t \mid \$^t = b_1 \$_{bi,1}^t + b_2 \$_{bi,2}^t + \dots + b_r \$_{bi,r}^t + c_1 \$_{uni,1}^t + c_2 \$_{uni,2}^t + \dots + c_p \$_{uni,p}^t, \quad (6) \\ \text{where } b_i \in (-\infty, \infty) \text{ and } c_j \in [0, \infty) \}.$$

Now that the set  $U$  has been formed, the local constraint surface can be defined by the twists on the boundary of  $U$ . Thus in order to compute the slope of the constraint surface, it is necessary to compute the slope of each twist on the boundary in  $U$ . While this would appear difficult, as the boundary of  $U$  is formed by an infinite number of twists, it is shown in [18] that only a small number of twists need to be considered in order to determine the stability of the pose.

### Modification for Redundant Manipulators

Note that for non-redundant cable robots  $p + r = n$ , where  $r$  was the dimension of the nullspace of  $\mathbf{J}$  and  $n$  is the dimension of the task space. For a redundant manipulator, the procedure must be modified slightly. If there are  $p$  cables and the dimension of the task space is  $n$  and  $p > n$ , then the modified  $\mathbf{J}$ s must be formed by removing  $(p - n + 1)$  rows at a time. For additional details see [18].

## V. STABILITY MEASURE

Once  $U$  has been formed, this set can be used to compute the resulting stability of the pose. The slope of the twists in  $U$  that define the constraint surface can be calculated in a straightforward manner if the units in all dimensions are identical, as was the case for the example point-mass end-effector discussed earlier. However, for twists in mixed-dimensional spaces slope is not defined. Here the definition of slope will be extended to *generalized slope* for mixed-dimensional twists by considering the kinetic energy of the end-effector as it undergoes that twist.

### A. Motivation

Consider again the manipulator in Figure 3. Applying the procedure described in Section IV to this manipulator results in  $U = \{ \$^t \mid \$^t = c_1 \vec{v}_1 + c_2 \vec{v}_2 \}$ . Consider giving the end-effector an instantaneous velocity of  $\alpha \vec{v}_1$  where  $\alpha > 0$ . Given the end-effector has mass  $m$ , the resulting kinetic energy of the end-effector is:

$$T = \frac{1}{2} m (\alpha \|\vec{v}_1\|)^2 \quad (7)$$

$$= \frac{1}{2} m (\alpha |v_{1,x}|)^2 + \frac{1}{2} m (\alpha |v_{1,y}|)^2 \quad (8)$$

where in (8) the energy has been split into two components, one due to velocity in the horizontal direction and one due to velocity in the vertical direction. If the ratio of these components is evaluated, a convenient result occurs:

$$\frac{\frac{1}{2} m (\alpha |v_{1,y}|)^2}{\frac{1}{2} m (\alpha |v_{1,x}|)^2} = \frac{|v_{1,y}|^2}{|v_{1,x}|^2} = s_1^2 \quad (9)$$

Thus the square of the slope of the first constraint surface can be determined by taking the ratio of the ‘‘vertical’’ kinetic energy associated with a velocity along  $\vec{v}_1$  to the ‘‘horizontal’’ kinetic energy associated with the same velocity.

While the example shown here was a very simple scenario, this concept of slope as a function of energy ratios can be extended to mixed-dimensional space, but can be more clearly understood by considering a mapping of twists and wrenches to an intermediate space.

### B. Intermediate Space

Without loss of generality, the origin of the coordinate frame can be placed at  $G$  with the axes aligned with the principle axes of the end-effector. A mapping can then be defined between the mixed-dimensional task space and an intermediate space that has linear dimensions only. A mixed-dimensional twist  $\$i^t$  can be mapped to a generalized velocity  $\hat{v}_i$

$$\hat{v}_i = \mathbf{A} \$i^t \quad (10)$$

where

$$\mathbf{A} = \begin{bmatrix} I^{\ell \times \ell} & 0 & \cdots & 0 \\ 0 & \rho_1 & \cdots & 0 \\ \vdots & \vdots & \ddots & \vdots \\ 0 & 0 & \cdots & \rho_{(n-r)} \end{bmatrix} \quad (11)$$

where there are  $\ell$  linear dimensions in the task space,  $I$  is the identity matrix and  $\rho_i$  is the radius of gyration of the end-effector about axis  $i$ .

A mixed-dimensional wrench  $\mathbb{S}_j^w$  can be mapped to a generalized force  $\hat{f}_j$

$$\hat{f}_j = \mathbf{B} \mathbb{S}_j^w \quad (12)$$

where

$$\mathbf{B} = \mathbf{A}^{-1} = \begin{bmatrix} I^{\ell \times \ell} & 0 & \cdots & 0 \\ 0 & \frac{1}{\rho_1} & \cdots & 0 \\ \vdots & \vdots & \ddots & \vdots \\ 0 & 0 & \cdots & \frac{1}{\rho_{(n-r)}} \end{bmatrix} \quad (13)$$

This mapping is essentially using the radii of gyration as characteristic lengths for the corresponding rotation elements of the twists and wrenches. As a result, the intermediate space of  $\hat{v}_i$  and  $\hat{f}_j$  has some nice properties. First, the dot product between a generalized velocity and a generalized force is equal to the power product between the corresponding twist and wrench:

$$\hat{v}_i^T \hat{f}_j = \{\mathbb{S}_i^t\}^T \mathbf{A}^T \mathbf{B} \mathbb{S}_j^w = \{\mathbb{S}_i^t\}^T \mathbb{S}_j^w \quad (14)$$

Secondly, the magnitude of a generalized velocity is proportional to the kinetic energy of the end-effector undergoing the corresponding twist. For compactness, define the kinetic energy  $T$  of a twist  $\mathbb{S}^t$  as:

$$T(\mathbb{S}^t) = \frac{1}{2} (\mathbb{S}^t)^T \mathbf{M}(\mathbb{S}^t) \quad (15)$$

where  $\mathbf{M} = \mathbf{A}^2 m$  is the inertia matrix of the end-effector. Then:

$$\begin{aligned} T(\mathbb{S}_i^t) &= \frac{m}{2} (\mathbb{S}_i^t)^T \mathbf{A}^2 (\mathbb{S}_i^t) \\ &= \frac{m}{2} (\mathbf{A} \mathbb{S}_i^t)^T (\mathbf{A} \mathbb{S}_i^t) = \frac{m}{2} \|\vec{v}_i\|^2 \end{aligned} \quad (16)$$

Thus in this intermediate space vector operations can be performed that are not defined for mixed-dimensional space, but retain physical meaning when mapped back to the mixed-dimensional task space. Note, however, that there does not appear to be any physical meaning associated with the magnitude of  $\hat{f}_j$ . An illustration of generalized forces and velocities is shown in Figure 5.

### C. Generalized Slope

If the set  $U$  is mapped to this space via  $\mathbf{A}$ , the twists now have consistent units and the ‘‘slope’’ of these twists can be calculated. In order to calculate the slope of a twist, it must be decomposed into a component ‘‘parallel’’ to the gravitational wrench and a component ‘‘perpendicular’’ to the gravitational wrench. We must be careful to properly define what we mean by parallelism here, as orthogonality and parallelism are

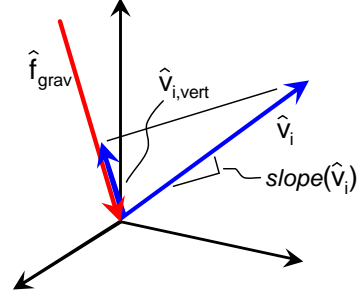


Fig. 5. Generalized force and velocities in the intermediate space.

ordinarily not defined between twists and wrenches. Rather, the vertical component of a twist (‘‘parallel’’ to gravity) can be defined as follows. Assume a known gravitational wrench  $\mathbb{S}_{grav}^w$ . For a given twist  $\mathbb{S}_i^t$ , its vertical component is the twist  $\mathbb{S}_{i,vert}^t$  that satisfies

$$T(\mathbb{S}_{i,vert}^t) = \min_{\{\mathbb{S}_j^t\}^T \mathbb{S}_{grav}^w = \{\mathbb{S}_i^t\}^T \mathbb{S}_{grav}^w} T(\mathbb{S}_j^t) \quad (17)$$

That is, of all the twists that have the same power product with  $\mathbb{S}_{grav}^w$  as  $\mathbb{S}_i^t$ ,  $\mathbb{S}_{i,vert}^t$  is the twist that results in the lowest kinetic energy of the end-effector. While this twist may be difficult to find, in the intermediate space defined here this twist is easy to construct. The twist  $\mathbb{S}_i^t$  can be mapped to  $\hat{v}_i$  and the wrench  $\mathbb{S}_{grav}^w$  can be mapped to  $\hat{f}_{grav}$ .

$$\hat{v}_i = \mathbf{A} \mathbb{S}_i^t \quad (18)$$

$$\hat{f}_{grav} = \mathbf{B} \mathbb{S}_{grav}^w \quad (19)$$

If the mapping of  $\mathbb{S}_{i,vert}^t$  is denoted  $\hat{v}_{i,vert}$  the relationship described in (17) can be rephrased as follows. In the intermediate space,  $\hat{v}_{i,vert}$  is the shortest vector that has the same dot product with  $\hat{f}_{grav}$  as  $\hat{v}_i$ . Thus by simple geometry it is easy to see that  $\hat{f}_{grav}$  and  $\hat{v}_{i,vert}$  are parallel. Thus to construct  $\mathbb{S}_{i,vert}^t$ , project  $\hat{v}_i$  onto  $\hat{f}_{grav}$  as shown in Figure 5 and map this velocity back into the twist space:

$$\hat{v}_{i,vert} = \frac{\hat{f}_{grav}}{\|\hat{f}_{grav}\|^2} \hat{f}_{grav} \cdot \hat{v}_i \quad (20)$$

$$\mathbb{S}_{i,vert}^t = \mathbf{A}^{-1} \hat{v}_{i,vert} \quad (21)$$

The generalized slope ( $GS$ ) of the twist is then defined as the slope of the corresponding generalized velocity:

$$GS(\mathbb{S}_i^t) = slope(\hat{v}_i) = \frac{\|\hat{v}_{i,vert}\|}{\|\hat{v}_i - \hat{v}_{i,vert}\|}. \quad (22)$$

Because of the relationship in (16) between the magnitude of generalized velocities and the kinetic energy of the end-effector,  $GS(\mathbb{S}_i^t)$  can be expressed as:

$$GS(\mathbb{S}_i^t)^2 = \frac{T(\mathbb{S}_{i,vert}^t)}{T(\mathbb{S}_i^t - \mathbb{S}_{i,vert}^t)} = \frac{T(\mathbb{S}_{i,vert}^t)}{T(\mathbb{S}_i^t) - T(\mathbb{S}_{i,vert}^t)}. \quad (23)$$

Note that the last equality in (23) is true because  $\mathbb{S}_i^t$  and  $\mathbb{S}_{i,vert}^t$  are orthogonal with respect to  $\mathbf{M}$ .

Using this approach, the generalized slope of the twists in  $U$  can be computed and the slope-based stability measure can

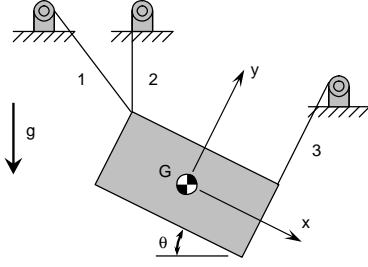


Fig. 6. Stability Calculation Example.

now be defined for general spatial underconstrained cable-driven robots. The stability  $S$  of a pose  $P$  of an underconstrained cable robot is defined as:

$$S(P) = \min_{\mathcal{S}_i^t \in U} \frac{T(\mathcal{S}_{i,vert}^t)}{T(\mathcal{S}_i^t) - T(\mathcal{S}_{i,vert}^t)} \quad (24)$$

$$= \min_{\mathcal{S}_i^t \in U} GS(\mathcal{S}_i^t)^2. \quad (25)$$

By mapping  $U$  to the intermediate space (24) simplifies to:

$$S(P) = \min_{\hat{v}_i \in \hat{U}} (\text{slope}(\hat{v}_i))^2 \quad (26)$$

which is a generalization of (9).

Thus the stability of a pose is defined as the ratio of the kinetic energy associated with the “vertical” component of any twist in  $U$  to the remaining kinetic energy of the twist, minimized over all of the twists in  $U$ .

## VI. CALCULATING $S(P)$

With the given formulation for  $S(P)$ , it is necessary to find the twists in  $U$  with minimum slope. Finding this minimum would be very difficult if it was necessary to perform an exhaustive search in  $U$ . Fortunately, such a search is not necessary. Because the slope function is a concave function over the compact set  $U$ , the twist with the minimum slope must lie on the boundary of  $U$ , and more specifically must be a multiple of one of the twists that positively span  $U$ . In addition, a scalar multiple of a twist will have the same slope as the original twist. As a result, it is only necessary to evaluate the slopes of the twists  $\{\mathcal{S}_{null,1}^t, \mathcal{S}_{null,2}^t, \dots, \mathcal{S}_{null,r}^t, \mathcal{S}_{mod,1}^t, \mathcal{S}_{mod,2}^t, \dots, \mathcal{S}_{mod,p}^t\}$ . In fact, if any twist  $\mathcal{S}_{null,i}^t$  exists,  $S(P) = 0$ . Thus at most  $p$  different twists must be evaluated to determine  $S(P)$ . See [18] for a more detailed proof.

In order to demonstrate the application of this stability measure to a manipulator, the stability of a planar 3-DOF 3-cable manipulator is calculated at a given pose. Consider the manipulator shown in Figure 6, which is constrained to lie in the plane. The end-effector is a 2 m  $\times$  4 m rectangle with a mass of 100 kg and rotational inertia of  $\frac{500}{3} \text{kg} \cdot \text{m}^2$ . In the given pose the bottom edge has a slope of  $-\frac{1}{2}$  with respect to gravity (i.e.  $\tan \theta = \frac{1}{2}$ ). The origin of the  $x$ - $y$  coordinate frame is placed at  $G$ , with the axes parallel to the edges of the end-effector. While in a planar problem it would be possible to simply align the  $y$ -axis with gravity, the coordinate frame is aligned with the geometry of the end-effector to illustrate

how the coordinate frame would align with the principle axes of a spatial end-effector.

Forming  $J$  results in:

$$J = \begin{bmatrix} \frac{-2}{\sqrt{5}} & \frac{1}{\sqrt{5}} & 0 \\ \frac{-1}{\sqrt{5}} & \frac{2}{\sqrt{5}} & \frac{-3}{\sqrt{5}} \text{ m} \\ 0 & 1 & 2 \text{ m} \end{bmatrix}$$

Calculation of the gravitational wrench and  $U$  results in:

$$\mathcal{S}_{grav}^w = \begin{pmatrix} \frac{1}{\sqrt{5}} \\ \frac{-2}{\sqrt{5}} \\ 0 \end{pmatrix} 980 \text{ N} \quad \mathcal{S}_{1,uni}^t = \begin{pmatrix} -7 \text{ m} \\ -2 \text{ m} \\ 1 \end{pmatrix} \frac{1}{\text{s}}$$

$$\mathcal{S}_{2,uni}^t = \begin{pmatrix} 1 \text{ m} \\ 2 \text{ m} \\ -1 \end{pmatrix} \frac{1}{\text{s}} \quad \mathcal{S}_{3,uni}^t = \begin{pmatrix} 1 \text{ m} \\ 2 \text{ m} \\ 1 \end{pmatrix} \frac{1}{\text{s}}$$

where  $U = \{\mathcal{S}^t | \mathcal{S}^t = c_1 \mathcal{S}_{1,uni}^t + c_2 \mathcal{S}_{2,uni}^t + c_3 \mathcal{S}_{3,uni}^t\}$ . By applying equations (18) through (21) the vertical components of the twists can be formed. Here the twists were chosen such that they all have the same vertical components:

$$\mathcal{S}_{1,vert}^t = \mathcal{S}_{2,vert}^t = \mathcal{S}_{3,vert}^t = \frac{3}{5} \begin{pmatrix} -1 \text{ m} \\ 2 \text{ m} \\ 0 \end{pmatrix} \frac{1}{\text{s}}$$

Thus the generalized slope of each twist can be calculated as follows:

$$GS(\mathcal{S}_i^t) = \sqrt{\frac{T(\mathcal{S}_{i,vert}^t)}{T(\mathcal{S}_{i,uni}^t) - T(\mathcal{S}_{i,vert}^t)}} \quad (27)$$

where  $T(\mathcal{S}_{i,vert}^t)$  is  $90 \text{ kg} \frac{\text{m}^2}{\text{s}^2}$ . The generalized slopes of  $\mathcal{S}_{1,uni}^t$ ,  $\mathcal{S}_{2,uni}^t$  and  $\mathcal{S}_{3,uni}^t$  are then 0.1845, 0.608 and 0.608, respectively. The twist with the lowest generalized slope is  $\mathcal{S}_{1,uni}^t$ , resulting in  $S(P) = 0.1845^2 = 0.0340$ .

## VII. APPLICATIONS

The question remains as to how a manipulator can be described as stable or unstable considering that the stability of the poses of the manipulator can differ greatly from one pose to another. One approach involves examining the stability of poses of the robot within its desired task space (the positional and rotational space that the robot can reach statically and in which the robot is required to operate). The desired task space  $D$  can be discretized into a finite number of poses and the stability measure can be applied to each one of these poses, resulting in a scalar field of manipulator stability over the desired workspace. There are many possible ways to use this information to define the stability of the robot, but due to space limitations only one will be described. The *Minimum Stability Measure* is defined as:

$$S_{min} = \min_D S(P) \quad (28)$$

This measure characterizes the manipulator by its lowest possible stability in  $D$ , essentially providing the worst-case scenario for using the manipulator in this task space. Using this kind of measure to describe the overall stability of a cable robot, it is possible to now use that information to optimize

the robot by choosing optimal cable-mount locations or end-effector geometry. Note however that the way the stability of a particular pose is defined, there are some parameters which cannot be optimized using stability alone. For example, the mass of the end-effector cancels out of Equation (24) and thus cannot be optimized based on this analysis. Additional measures of overall stability are described in [18].

### VIII. DISCUSSION

The stability measure  $S(P)$  is, to the authors' knowledge, the first stability measure proposed for underconstrained cable robots. It has many advantageous characteristics. First, because the measure is based on slope, it is physically meaningful. Because the calculation of slope is energy-based, it is scale- and frame-invariant. The method of computing the stability is not only relatively easy, it is also flexible enough that it allows for stability to be computed in the presence of any constant external wrench, not just gravity. This can be accomplished by simply replacing  $\mathcal{S}_{grav}^w$  in all calculations with the net external wrench due to gravity and additional constant external wrenches.

The stability measure does have some drawbacks. First, using the stability measure to calculate the overall stability may be computationally time-consuming as the task space must be discretized and the stability measure applied at each of these poses. Secondly, the inertial properties of the end-effector must be known completely. This information may not be available if the end-effector picks up objects with unknown masses and dimensions. This measure is also limited to analyzing manipulators with single-body end-effectors. This may not always be the case, such as when a payload is suspended from the manipulator by a hook or additional cable. Lastly, it is not obvious what an acceptable minimum value is for  $S(P)$ . Experimentation and practical considerations may need to be taken into account to determine what constitutes an appropriate minimum necessary value of  $S(P)$  for a given manipulator. However, given such a value, it is possible to construct a *Minimum Stability Workspace*, the set of all poses of a manipulator where  $S(P)$  meets or exceeds the minimum required stability value.

### IX. CONCLUSION AND FUTURE WORK

In conclusion, the stability measure presented here is a slope-based measure of the stability of an underconstrained cable robot at a particular pose. Because the measure is based on slope, it has physical meaning. The measure is easy to compute and is flexible, allowing for stability to be computed in the presence of constant external wrenches other than gravity.

In order to better illustrate and understand the concepts behind the measure, an intermediate space was introduced. Vector operations within this space carry physical meaning and allow simplified computation of the twist "parallel" to gravity.

A simple method was presented for forming  $U$ , the set of all twists that the end-effector can instantaneously undergo without violating cable constraints. This set not only allows computation of the stability measure, but may also be useful by itself for future analysis of these manipulators.

Future work in this area will include expanding this analysis to determine the stability of multi-body end-effectors. In addition, finite displacement stability will be examined. This is expected to be more difficult, however, because it requires forming large portions of the constraint surface. Lastly, this analysis may be modified to include non-ideal effects such as cable stretch and sag.

### ACKNOWLEDGMENT

This research was supported by a National Defense Science and Engineering Graduate (NDSEG) Fellowship and National Science Foundation grant #CMS-9984279.

### REFERENCES

- [1] August Design, "SkyCam," [www.august-design.com](http://www.august-design.com).
- [2] —, "Intelligent spreader bar," [www.august-design.com](http://www.august-design.com).
- [3] J. Albus, R. Bostelman, and N. Dagalakis, "The NIST RoboCrane," *Journal of National Institute of Standards and Technology*, vol. 97, no. 3, May-June 1992.
- [4] R. Verhoeven, M. Hiller, and S. Tadokoro, "Workspace of tendon-driven stewart platforms: Basics, classification, details on the planar 2-dof class," in *Proceedings of the 4th International Conference on Motion and Vibration Control*, vol. 3, 1998, pp. 871–876.
- [5] A. Fattah and S. K. Agrawal, "Design of cable-suspended planar parallel robots for an optimal workspace," in *Proceedings of the Workshop on Fundamental Issues and Future Research Directions for Parallel Mechanisms and Manipulators*, Quebec City, Quebec, Canada, October 2002, pp. 195–202.
- [6] G. Barette and C. M. Gosselin, "Kinematic analysis and design of planar parallel mechanisms actuated with cables," in *Proceedings of the ASME 2000 Design Engineering Technical Conferences and Computers and Information in Engineering Conference (DETC'00)*, Baltimore, Maryland, September 2000.
- [7] Y. Shen, H. Osumi, and T. Arai, "Manipulability measures for multi-wire driven parallel mechanisms," in *Proceedings of the IEEE International Conference on Industrial Technology*, December 1994, pp. 550–554.
- [8] Y.-Q. Zheng and X.-W. Liu, "Force transmission index based workspace analysis of a six dof wire-driven parallel manipulator," in *Proceedings of ASME 2002 Design Engineering Technical Conferences and Computer and Information in Engineering Conference (DETC'02)*, Montreal, Canada, 2002, pp. 1–8.
- [9] P. Gallina and G. Rosati, "Manipulability of a planar wire driven haptic device," *Mechanism and Machine Theory*, pp. 215–228, 2002.
- [10] N. Yanai, M. Yamamoto, and A. Mohri, "Anti-sway control for wire-suspended mechanism based on dynamics compensation," in *Proceedings of the 2002 IEEE International Conference on Robotics and Automation*, Washington, D.C., May 2002, pp. 4287–4292.
- [11] A. B. Alp and S. K. Agrawal, "Cable suspended robots: Design, planning and control," in *Proceedings of the 2002 IEEE International Conference on Robotics and Automation*, Washington, D.C., 2002, pp. 4275–4280.
- [12] P. Bosscher and I. Ebert-Uphoff, "Wrench-based analysis of cable-driven robots," in *2004 IEEE International Conference on Robotics and Automation*, 2004.
- [13] S. Kawamura, W. Choe, S. Tanaka, and S. Pandian, "Development of an ultrahigh speed robot FALCON using wire drive system," in *Proceedings of the 1993 IEEE/ICRA International Conference on Robotics and Automation*, vol. 1, Nagoya, Japan, May 1995, pp. 215–220.
- [14] S. Kawamura and K. Ito, "A new type of master robot for teleoperation using radial wire drive system," in *Proceedings of the 1993 IEEE/RSJ International Conference on Intelligent Robots and Systems*, Yokohama, Japan, July 1993, pp. 55–60.
- [15] I. Ebert-Uphoff and P. A. Voglewede, "On the connections between cable-driven robots, parallel robots and grasping," in *2004 IEEE International Conference on Robotics and Automation*, 2004.
- [16] W. S. Howard and V. Kumar, "On the stability of grasped objects," *IEEE Transactions on Robotics and Automation*, vol. 12, no. 6, pp. 904–917, December 1996.
- [17] J. C. Trinkle, "On the stability and instantaneous velocity of grasped frictionless objects," *IEEE Transactions on Robotics and Automation*, vol. 8, no. 5, pp. 560–572, October 1992.
- [18] P. Bosscher and I. Ebert-Uphoff, "Stability measures for underconstrained cable-driven robots," *IEEE Transactions on Robotics and Automation*, in Preparation.